ANALYSIS OF UPPER RESPIRATORY TRACT SEGMENTATION FEATURES TO DETERMINE NASAL CONDUCTANCE

Oleg Avrunin[1], Yana Nosova[1], Nataliia Shushliapina[2], Ibrahim Younouss Abdelhamid[1], Oleksandr Avrunin[1], Svetlana Kyrylashchuk[3], Olha Moskovchuk[4], Orken Mamyrbayev[5]

[1]Kharkiv National University of Radio Electronics, Kharkiv, Ukraine, [2]Kharkiv National Medical University, Kharkiv, Ukraine, [3]Vinnytsia National Technical University, Vinnytsia, Ukraine, [4]Vinnytsia Mykhailo Kotsiubynskyi State Pedagogical University, Vinnytsia, Ukraine, [5]Institute of Information and Computational Technologies of the Kazakh National Technical University named after K. I. Satbayev, Almaty, Kazakhstan

Abstract. The paper examines the features of segmentation of the upper respiratory tract to determine nasal air conduction. 2D and 3D illustrations of the segmentation process and the obtained results are given. When forming an analytical model of the aerodynamics of the nasal cavity, the main indicator that characterizes the configuration of the nasal canal is the equivalent diameter, which is determined at each intersection of the nasal cavity. It is calculated based on the area and perimeter of the corresponding section of the nasal canal. When segmenting the nasal cavity, it is first necessary to eliminate air structures that do not affect the aerodynamics of the upper respiratory tract - these are, first of all, intact spaces of the paranasal sinuses, in which diffuse air exchange prevails. In the automatic mode, this is possible by performing the elimination of unconnected isolated areas and finding the difference coefficients of the areas connected by confluences with the nasal canal in the next step. High coefficients of difference of sections between intersections will indicate the presence of separated areas and contribute to their elimination. The complex configuration and high individual variability of the structures of the nasal cavity does not allow segmentation to be fully automated, but this approach contributes to the absence of interactive correction in 80% of tomographic datasets. The proposed method, which takes into account the intensity of the image elements close to the contour ones, allows to reduce the averaging error from tomographic reconstruction up to 2 times due to artificial sub-resolution. The perspective of the work is the development of methods for fully automatic segmentation of the structures of the nasal cavity, taking into account the individual anatomical variability of the upper respiratory tract.

Keywords: aerodynamics of nasal breathing, nasal cavity, tomographic reconstruction, segmentation, upper respiratory tract, air conduction

ANALIZA CECH SEGMENTACJI GÓRNYCH DRÓG ODDECHOWYCH W CELU OKREŚLENIA PRZEWODNICTWA NOSOWEGO

Streszczenie. W pracy przeanalizowano cechy segmentacji górnych dróg oddechowych w celu określenia powietrznego przewodnictwa nosowego. Przedstawiono zdjęcia 2D i 3D procesu segmentacji oraz uzyskanych wyników. Podczas formowania analitycznego modelu aerodynamiki jamy nosowej głównym wskaźnikiem charakteryzującym konfigurację kanału nosowego jest ekwiwalentna średnica, którą wyznacza się na każdym skrzyżowaniu jam nosowych. Jest ona obliczana na podstawie pola powierzchni i obwodu odpowiedniego odcinka kanału nosowego. Podczas segmentacji jamy nosowej w pierwszej kolejności należy wyeliminować struktury powietrzne, które nie wpływają na aerodynamikę górnych dróg oddechowych – są to przede wszystkim nienaruszone przestrzenie zatok przynosowych, w których dominuje rozproszona wymiana powietrza. W trybie automatycznym jest to możliwe dzięki eliminacji niepołączonych izolowanych obszarów i znalezieniu, w kolejnym kroku, współczynników różnicy obszarów połączonych konfluencjami z przewodem nosowym. Wysokie współczynniki różnic przekrojów pomiędzy skrzyżowaniami będą wskazywały na obecność wydzielonych obszarów i przyczynią się do ich eliminacji. Złożona konfiguracja i duża zmienność osobnicza struktur jamy nosowej nie pozwala na pełną automatyzację segmentacji, jednak takie podejście przyczynia się do braku konieczności interaktywnej korekcji w 80% zestawów danych tomograficznych. Zaproponowana metoda, uwzględniająca intensywność elementów obrazu znajdujących się blisko konturu, pozwala na nawet 2-krotne zmniejszenie błędu uśredniania z rekonstrukcji tomograficznej, wynikającego ze sztucznej subrozdzielczości. Perspektywą pracy jest opracowanie metod w pełni automatycznej segmentacji struktur jamy nosowej z uwzględnieniem indywidualnej zmienności anatomicznej górnych dróg oddechowych.

Słowa kluczowe: aerodynamika oddychania przez nos, jama nosowa, rekonstrukcja tomograficzna, segmentacja, górne drogi oddechowe, przewodzenie powietrza

Introduction

Over the past 20 years, evidence-based medicine approaches have been established in the treatment and diagnostic procedures. Such evidentiary studies are based on the objectification of application based on quantitative instrumental methods and statistically reliable results. Thus, given the lack of hard standards for medical data, there are still many unsolved questions about the reliability of the obtained results, especially when conducting functional studies. One of the main tasks of modern medicine is to determine the dependence between the anatomical and functional properties of organs and their respective individual variability. In rhinology, such studies are conducted to analyze the functional indicators of nasal breathing and the architecture of the upper respiratory tract [13]. This is especially important when changing the configuration of intranasal structures during corrective surgical interventions to improve nasal air conduction in cases of nasal membrane distortions, chronic sinusitis, and other nosologies of functional rhinology [18]. At the same time, mathematical modeling allows predicting the results of operative interventions and carrying out their planning in virtual mode.

X-ray computed tomography and its modifications, such as spiral and cone-beam tomography [7, 18], are the main method of endoscopic diagnosis of the state of the upper respiratory tract. Taking into account the relatively small prevalence of the methods of functional testing of nasal breathing - rhinomanometry, the low repeatability of data and the absence of clear standards of some indicators in different conditions, types and methods of research,

at this stage the task of adding functional information to the results of computed tomography examinations [17, 23, 31]. For this, it is necessary to clearly define the configuration of the airways of the nasal cavity and build an aerodynamic model of the air flow during breathing on its basis [10, 24]. The design of aerodynamic models for channels with a complex configuration always involves the precision determination of the geometric shape of their walls, in particular, this applies to biological objects with high anatomical variability. Therefore, an urgent task is to study the peculiarities of the segmentation of the upper respiratory tract sections according to computer tomography data.

The purpose of the work is to study the features of the segmentation of the upper respiratory tract to determine nasal conduction.

1. Analysis of literature

Well-known specialists in the field of rhinology [13, 24] are dedicated to research in the field of nasal aerodynamics in the diagnosis of diseases of the upper respiratory tract. The latest data were the study of the characteristics of the nasal cavity using CFD methods and the verification of modeling results with clinical signs, as well as the prediction of functional results in rhinosurgery [8, 9]. The planning approaches of functional operative rhinosurgical interventions are being improved [20, 27]. The influence of the anatomical structure and changes in the architecture of the nose on the aerodynamics of the nasal cavity [11, 28], odontogenic sinusitis [18, 21], and sleep apnea syndrome

[2, 15], is being investigated. The simulation of the nasal cavity and the corresponding study of the characteristics of the air flow during breathing are carried out [6, 22].

Many works [24] are also dedicated to the methods of functional testing of nasal breathing, in particular to the methods of front [10, 24] and rear active rhinomanometry, which allow obtaining data on the coefficient of aerodynamic nasal resistance in different breathing modes. The principles of construction of rhinomanometry equipment and features of its use are considered, in particular, errors in the measurement of respiratory parameters. Evidential studies of respiratory and olfactory function are being conducted [5, 12, 29]. The issues of acoustic rhinometry in the non-invasive determination of the configuration of the nasal cavity [8, 26, 30] and natural 3D modeling of the upper respiratory tract [4, 19] and intelligent analysis of geometric data [14] are also considered. These approaches make it possible to study the personalized functional capacity of the upper respiratory tract to pass air in certain breathing modes, as well as to conduct an analysis of the adequacy of therapy [8, 27].

In general, the vast majority of approaches to studying the aerodynamics of the upper respiratory tract are aimed at building CFD models and their virtual tests. For this, various methods are used to obtain the configuration of the nasal cavity, such as X-ray computed tomography (the most common) and other medical imaging methods, such as acoustic rhinometry. The latter is non-invasive (does not involve X-ray radiation), but in some cases, due to overprints, it causes a large error in determining the boundaries of the airways. In recent years, after the widespread introduction of 3D prototyping methods, the approach of printing personalized full-scale models of the nasal cavity and testing them on aerodynamic stands to determine the corresponding pressure losses has been adopted. But the high adequacy of full-scale modeling of the nasal cavity is possible only when printing models that fully imitate the properties of both the mucous membrane and the mobile structures of the external nose, which requires the use of different materials for printing and complicates the process of making such models. The authors propose a discrete mathematical model of one-dimensional air flow in the nasal cavity, which allows analytically and more visually to investigate the coefficient of aerodynamic nasal resistance in each cross-section according to its equivalent hydraulic diameter. The reliability of such simulations, both CFD and natural, depends on the correct definition of the configuration of the nasal cavity. However, the peculiarities of creating aerodynamic models of the upper respiratory tract, the construction of which directly depends on the accuracy of the presentation of the geometric configuration of the nasal cavity, remain unsolved issues [1, 3].

Therefore, it is appropriate to consider the features of the segmentation of the airways of the nasal cavity for the construction of aerodynamic models for determining nasal conductivity [28].

2. Materials and methods

X-ray spiral computed tomography SOMATOM + E-motion of SIEMENS firm (Germany) on the basis of the Otorhinolaryngology Department of the Kharkiv Regional Clinical Hospital was used for endoscopic studies. Scanning was performed parallel to the orbito-meatal line with a step of 1 mm between slices and a spatial resolution in the slice plane of 0.4 mm. The raw data were obtained in DICOM format with the image size of slices 512×512 elements. Next, multiplanar reconstructions were performed in the frontal plane with a step of 2 mm parallel to the sections that are perpendicular to the air flow throughout the nasal cavity during breathing. An analytical model of one-dimensional air flow in the nasal cavity was used to build the aerodynamic model.

The error of the tomographic reconstruction on the used equipment was 0.2 mm (half of the voxel size in the slice plane). This is approximately 2% of the typical linear size (10 mm)

of nasal airway cross-sections on most slices. The error in the frontal reconstruction is 1 mm in the distance between the slices, the error in the vertical direction is 0.5 mm (approximately 5% of the measured characteristic size).

Analytical determination of the coefficient of aerodynamic resistance of the nasal cavity is based on the assumption that the airways of the nose are considered as two parallel channels. The total air flow is the sum of the flow through the left Q_L and right Q_R nasal passages, respectively.

$$Q_\Sigma = Q_L + Q_R \qquad (1)$$

and the pressure drops are the same for the left Δp_L and right Δp_R nasal canals.

$$\Delta p = \Delta p_L = \Delta p_R \qquad (2)$$

At the same time, the nasal cavity is divided into sections that are perpendicular to the air flow, and the total pressure losses along the length $\sum \Delta p_{l_L}$, $\sum \Delta p_{l_R}$ and local (r-regional) $\sum \Delta p_{r_L}$, $\sum \Delta p_{r_R}$ are the sums of these resistances in each section. Therefore, in accordance with expression (1), taking into account the quadratic dependence of the pressure drop Δp on the air flow rate Q in the turbulent flow regime under most breathing modes, the pressure drops through each nasal passage will be determined by the following formulas [6, 7]

$$\Delta p_L = Q_L^2 A_L = \sum \Delta p_{l_L} + \sum \Delta p_{r_L} =$$
$$= \sum \lambda_L \cdot \rho \frac{L_L}{d_{e_L}} \frac{Q_L^2}{2 S_L^2} + \sum \xi_L \cdot \rho \frac{Q_L^2}{2 S_L^2} \qquad (3)$$

$$\Delta p_R = Q_R^2 A_R = \sum \Delta p_{l_R} + \sum \Delta p_{r_R} =$$
$$= \sum \lambda_R \cdot \rho \frac{L_R}{d_{e_R}} \frac{Q_R^2}{2 S_R^2} + \sum \xi_R \cdot \rho \frac{Q_R^2}{2 S_R^2} \qquad (4)$$

where λ_L, λ_R are the Darcy coefficients (pressure loss along the length) for the left and right nasal passages, respectively;

ξ_L, ξ_R are local resistance coefficients for the left and right nasal passages, respectively;

L_L, L_R are the lengths of the left and right nasal passages, respectively;

Q_L, Q_R – air flow through the left and right nasal passages, respectively;

ρ – air density;

d_{e_L}, d_{e_R} are the equivalent diameters of the left and right nasal passages, respectively, which are expressed for each intersection of the left and right nasal canals with the planes S_L, S_R and P_L, P_R perimeters, respectively, according to the formula, where $*$ is replaced by L and R

$$d_{e_*} = \frac{4 S_*}{P_*} \qquad (5)$$

A_L, A_R – coefficients of aerodynamic nasal resistance for the left and right nasal channels, which are determined from formulas (3), (4) and (5) as

$$A_L = \sum \lambda_L \cdot \rho \frac{L_L}{d_{e_L} \cdot 2 S_L^2} + \sum \xi_L \cdot \rho \frac{1}{2 S_L^2} \qquad (6)$$

$$A_R = \sum \lambda_R \cdot \rho \frac{L_R}{d_{e_R} \cdot 2 S_R^2} + \sum \xi_R \cdot \rho \frac{1}{2 S_R^2} \qquad (7)$$

Figure 1 shows typical segmented cross-sections of the airways of the nasal cavity with a location near the nose (Fig. 1a), in the central area (Fig. 1b) and at the exit to the nasopharynx (Fig. 1c).
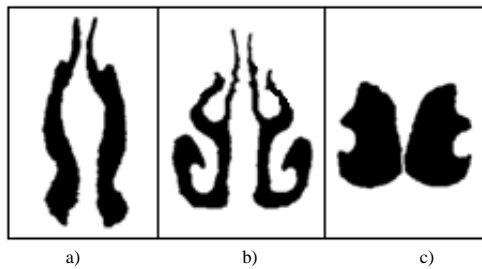
Fig. 1. Typical segmented cross-sections of the airways of the nasal cavity with the location: a) near the crown; b) in the central area; c) when exiting the nasopharynx

Based on the fact that in the proposed model it is not possible to take into account the mutual influence of local resistances, only the largest of them is determined. The overall coefficient of aerodynamic nose drag was determined as with the parallel connection of two air ducts.

3. Results and discussion

From the above formulas (4)-(7) and taking into account the complexity of the configuration of the air channels of the nasal cavity in Fig. 1, it is obvious that the accuracy of determining the coefficients of aerodynamic nasal resistance depends on the accuracy of determining the parameters of the sections of the nasal passages, in particular the area and equivalent diameter. Therefore, special attention is paid to their definition when creating a mathematical model of the nasal cavity. Segmentation of the air regions of the upper respiratory tract on tomographic multiplanar reconstructive slices $B(x, y)$ is carried out according to the threshold level T, which corresponds to the air density in HU numbers, or directly according to the minimum level of brightness when setting the parameters of the soft tissue window of tomographic visualization.

$$F(x, y) = \begin{cases} 1; & B(x, y) \leq T \\ 0; & B(x, y) > T \end{cases} \qquad (8)$$

where $F(x, y)$ is the binary characteristic function of air regions

An example of building a binary characteristic function of air regions for a tomographic section in figure 2a is given in figure 2b.

Fig. 2. Illustration of the segmentation of the frontal section of the nasal cavity: a) input tomographic section; b) binary characteristic function of air regions

A three-dimensional visualization of the segmented airways of the nasal cavity is shown in figure 3. The original image clearly shows cavities containing air, but not all of them (for example, paranasal sinuses, conchobuloses) directly affect the aerodynamic processes in the upper respiratory tract and should be removed from the model, which will be discussed later. Determining contours of segmented structures is performed on already obtained binary images using differential operators

$$A_{px} = \begin{pmatrix} 1 & 0 \\ 0 & -1 \end{pmatrix}; \quad A_{py} = \begin{pmatrix} 0 & 1 \\ -1 & 0 \end{pmatrix} \qquad (9)$$

or structured elements, or logical conditions of boundary features.

Fig. 3. Volumetric visualization of the segmented airways of the nasal cavity

A contour segmented image of the right half of the nasal cavity is shown in figure 4a. Figure 4b shows the corresponding contour image after thinning the border and removing unnecessary corner elements of the border according to the illustration in figure 5.
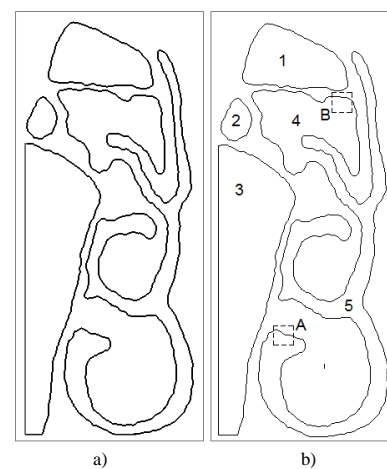

Fig. 4. Illustration of the process of contour segmentation of the right half of the nasal cavity on the tomographic section from figure 2: a) input image after contour segmentation; b) the corresponding contour image after thinning the border and removing unnecessary corner elements of the border with designations of areas belonging to anatomical structures with designations (1, 2, 4 – cells of the clavicle, 3 – fragment of the maxillary sinus; 5 – nasal passage; A – designation of the area in lower nasal passage, B is the designation of the area in the cells of the ethmoid bone)

A contour model of nasal airway slices is shown in figure 6.

The algorithm for building a the contour model based on frontal multiplanar tomographic reconstructions is reduced to the following steps:

- segmentation of air cavities by intensity threshold;
- logical filtering of separate unconnected local disturbances of a small area and cavities that do not participate in aerodynamic processes, according to the method of determining the coefficients of difference of sections of segmented areas on different sections;
- processing of a segmented image by gradient operators;
- morphological post-processing to thin contours and eliminate discretization errors when determining the perimeter of the intersections.

As mentioned earlier, the main problem for fully automated segmentation of such data is that cavities that do not affect nasal aerodynamics remain in the output images. Their elimination can be carried out in the following sequential steps: perform multi-valued segmentation and eliminate unrelated objects (cells of the ethmoid bone with numbers 1, 2 and maxillary sinus 3) according to the example in figure 4b. But, if the obtained frontal tomographic section is located in the plane of the conjuncture of the parasinus (object 4 in Fig. 4b) and is directly connected to the airways of the nasal cavity (area 5 in Fig. 4b), then difficulties arise in its elimination.
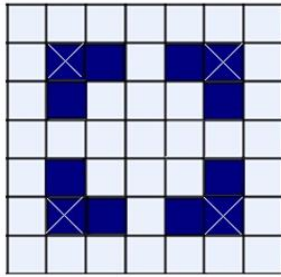
Fig. 5. Schematic illustration of the elimination of unnecessary corner elements of the border (indicated by hatching)

Performing successive operations of erosion and augmentation of areas to eliminate the co-mouth may not provide the required result with certain anatomical features and close values of the width of the co-mouth and the corresponding section of the nasal passage, as shown in the example from figures 2 and 4. Therefore, a differential technique is proposed at the next step, which takes into account the presence/absence of separate sections of objects at adjacent frontal intersections. At the same time, the coefficient of difference is calculated for each averaged section of the segmented upper respiratory tract for adjacent intersections with numbers *n* and *n-1*

$$k_n = M_n - M_{n-1} \tag{10}$$

where M_n and M_{n-1} are the averaged values of the characteristic function of image sections at adjacent intersections with numbers *n* and *n-1*, respectively. It is advisable to take the sizes of the plots as 3×3. Taking into account the absence of significant changes in the configuration of the nasal passages during the preliminary elimination of unrelated components of the paranasal sinuses on most sections, it is possible to deduce the empirical value of the difference coefficient threshold for areas that are absent on adjacent sections, which will be 0.25.
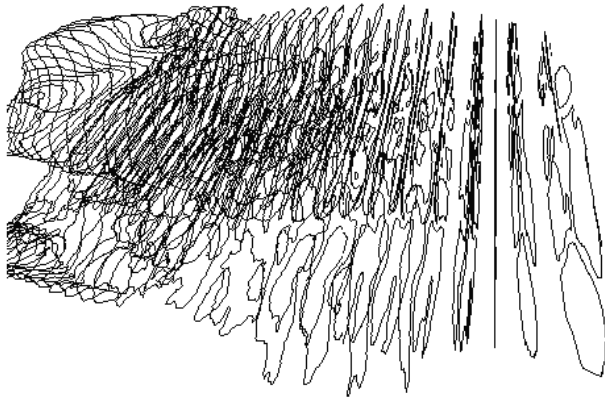

Fig. 6. Contour model of sections of the airways of the nasal cavity

An illustration of the values of the coefficient of difference k for sections A and B at the intersection with number n=24 is shown in figure 7. For the region of the lower nasal passage (A), the value of the coefficient of difference k is less than 0.25 and the section is correctly segmented; for the area of the accessory sinus of the ethmoid bone, the difference will be high (more than 0.9) due to the absence of the non-connected area of the sinus removed at the previous stage on the adjacent section. It is advisable to carry out the above calculations on the data of the binary characteristic function (Fig. 2b), the sections in Fig. 4b are shown for clarity. Based on the analysis of 110 tomographic datasets of the upper respiratory tract, manual actions during segmentation were performed in 23 cases, which was approximately 20%. At the same time, the main interactive operations were exclusion from the configuration of the model of various anatomical

structures, in most cases – cells of the reticular labyrinth and correction of fine structures in the area of the upper nasal passage. With an average width of the nasal canal of about 10 mm, the spatial tomographic resolution is 0.4 mm, which immediately provides an error in determining diametrically opposite walls of about 8%.
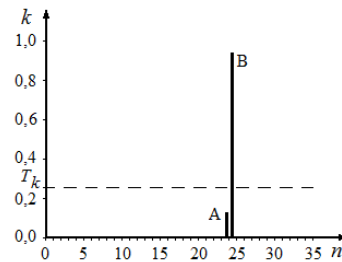

Fig. 7. Illustration of the values of the coefficient of difference k for sections A and B in figure 4, b (n – numbers of frontal intersections)

At the same time, it is expedient to use an algorithm that artificially increases the resolution by 2 times and performs manipulations on the image with the intensity of elements at sub-resolution according to the illustration in figure 8. According to this figure, at sub-resolution, an image element with intensity $B(x, y)$, which is in the border region to of a well-defined area with air, is divided into near $(x_n^{(s)}, y)$ and far $(x_f^{(s)}, y)$ elements during sub-resolution with the corresponding intensities $b(x_n^{(s)}, y)$ and $b(x_f^{(s)}, y)$.
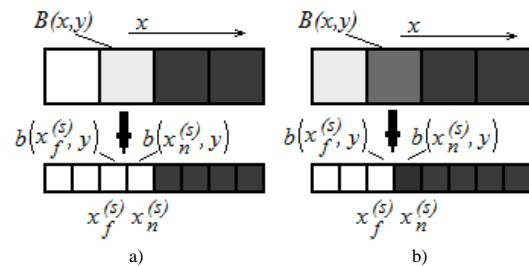

Fig. 8. Illustration of obtaining the intensity values of the contour elements of the image during the sub-resolution procedure ($B(x, y)$ input intensity of the input element of the image located in the boundary region to a clearly defined area with air; sub-resolution into near $(x_n^{(s)}, y)$ and $(x_f^{(s)}, y)$ far elements with corresponding intensities $b(x_n^{(s)}, y)$ and $b(x_f^{(s)}, y)$)

Moreover, the intensity of the subdistinct element close to the air section will be determined as

$$b(x_n^{(s)}, y) = \begin{cases} 1; & B(x, y) \le T_s \\ 0; & B(x, y) > T_s \end{cases} \tag{11}$$

where T_s is the threshold intensity value of the input element of the image, which can be about 18% of the maximum intensity in the image.

This approach makes it possible to eliminate the error from averaging during tomographic reconstruction of the image and increase the accuracy of determining the contour elements of the image up to 2 times (up to 4 percent). Areas *S* and perimeters *P* for each section of the nasal cavity are determined on the resulting segmented images for substitution in formulas (3) – (7). The area is defined as the sum of all values of the binary characteristic function at the intersection, and the perimeter taking into account linear n_l and diagonally n_d located contour elements according to the formula

$$P = n_l + \sqrt{2} \cdot n_d \tag{12}$$

This allows to reduce the error due to the separate consideration of the diagonal elements of the rectangular raster. When determining the area, the relative value of such elements will be insignificant and their individual contribution can be ignored. The resulting visualization of the contour at the intersection of the nasal canal after image processing in figures 2 and 4 is shown in figure 9, a. The initial surface visualization of both nasal channels is shown in figure 9b.

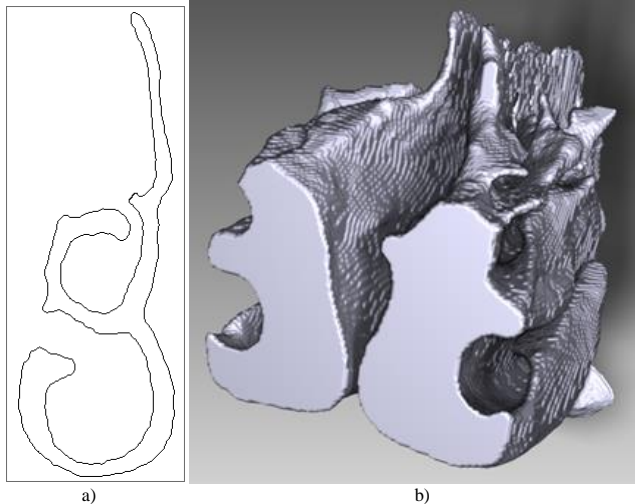a)   b)

Fig. 9. An example of the segmentation of the contours of the nasal canals: a) the resulting cross section of the nasal canal after image processing in figures 2 and 4; b) initial surface visualization of both nasal passages

4. Conclusions

When forming an analytical model of the aerodynamics of the nasal cavity, the main indicator that characterizes the configuration of the nasal canal is the equivalent diameter, which is determined at each intersection of the nasal cavity. It is calculated based on the area and perimeter of the corresponding section of the nasal canal. When segmenting the nasal cavity, it is first necessary to eliminate air structures that do not affect the aerodynamics of the upper respiratory tract – these are, first of all, intact spaces of the paranasal sinuses, in which diffuse air exchange prevails. In the automatic mode, this is possible by performing the elimination of disconnected isolated areas and finding the difference coefficients of the areas connected by mouths to the nasal canal in the next step. High coefficients of difference of sections between intersections will indicate the presence of separated areas and contribute to their elimination. The complex configuration and high individual variability of the structures of the nasal cavity does not allow segmentation to be fully automated, but this approach contributes to the absence of interactive correction in 80% of tomographic datasets. The proposed method, which takes into account the intensity of the image elements close to the contour ones, allows to reduce the averaging error from tomographic reconstruction up to 2 times due to artificial sub-resolution. The perspective of the work is the development of methods for fully automatic segmentation of the structures of the nasal cavity taking into account the individual anatomical variability of the upper respiratory tract.

References

[1] Aras A. et al.: Dimensional changes of the nasal cavity after transpalatal distraction using bone-borne distractor: an acoustic rhinometry and computed tomography evaluation. J. Oral Maxillofac. Surg. 68(7), 2010, 1487–1497.

[2] Avrunin O. G. et al.: Features of image segmentation of the upper respiratory tract for planning of rhinosurgical surgery. Paper presented at the 2019 IEEE 39th International Conference on Electronics and Nanotechnology, ELNANO 2019, 485–488.

[3] Avrunin O. G. et al.: Principles of computer planning in the functional nasal surgery. Przeglad Elektrotechniczny 93(3), 2017, 140–143 [http://doi.org/10.15199/48.2017.03.32].

[4] Avrunin O. G. et al.: Study of the air flow mode in the nasal cavity during a forced breath. Proc. of SPIE 10445, 2017 [http://doi.org/10.1117/12.2280941].

[5] Avrunin O. G. et al.: Possibilities of Automated Diagnostics of Odontogenic Sinusitis According to the Computer Tomography Data. Sensors 21, 1198, 2021 [http://doi.org/10.3390/s21041198].

[6] Berger M. et al.: Agreement between rhinomanometry and computed tomography-based computational fluid dynamics. International Journal of Computer Assisted Radiology and Surgery 16(4), 2021, 629–638 [http://doi.org/10.1007/s11548-021-02332-1].

[7] Cankurtaran M. et al.: Acoustic rhinometry in healthy humans: accuracy of area estimates and ability to quantify certain anatomic structures in the nasal cavity. Ann Otol. Rhinol. Laryngol. 116(12), 2007, 906–916.

[8] Churchill S. E. et al.: Morphological Variation and Airflow Dynamics in the Human Nose. Am. J. Of Hum. Biol. 16, 2004, 625–638.

[9] Cilluffo G., et al.: Assessing repeatability and reproducibility of anterior active rhinomanometry (AAR) in children. BMC Medical Research Methodology 20(1), 2020 [http://doi.org/10.1186/s12874-020-00969-1].

[10] Clement P. A.: Standardisation Committee on Objective Assessment of the Nasal Airway. Consensus report on 43, 2005, 169–179.

[11] Fyrmpas G. et al.: The value of bilateral simultaneous nasal spirometry in the assessment of patients undergoing. Rhinology 49(3), 2011, 297–303.

[12] Hsu Y. et al.: Role of rhinomanometry in the prediction of therapeutic positive airway pressure for obstructive sleep apnea. Respiratory Research 21, 2020, 115 [http://doi.org/10.1186/s12931-020-01382-4].

[13] Kang Y. J. et al.: The diagnostic value of detecting sudden smell loss among asymptomatic COVID-19 patients in early stage: The possible early sign of COVID-19. Auris Nasus Larynx 47(4), 2020, 565–573 [http://doi.org/10.1016/j.anl.2020.05.020].

[14] Kirichenko L. et al.: Machine learning in classification time series with fractal properties. Data 4(1), 2019, 5 [http://doi.org/10.3390/data4010005].

[15] Kuo C. J. et al.: Application of intelligent automatic segmentation and 3D reconstruction of inferior turbinate and maxillary sinus from computed tomography and analyze the relationship between volume and nasal lesion. Biomedical Signal Processing and Control 57, 2020, 101660 [http://doi.org/10.1016/j.bspc.2019.101660].

[16] Li C. et al.: Nasal structural and aerodynamic features that may benefit normal olfactory sensitivity. Chemical Senses 43(4), 2018, 229–237.

[17] Mlynski G. et al.: Correlation of nasal morphology and respiratory function. Rhinology 39(4), 2001, 197–201.

[18] Moghaddam M. G.et al.: Virtual septoplasty: A method to predict surgical outcomes for patients with nasal airway obstruction. International Journal of Computer Assisted Radiology and Surgery 15(4), 2020, 725–735 [http://doi.org/10.1007/s11548-020-02124-z].

[19] Ohlmeyer S. et al.: Cone beam CT imaging of the paranasal region with a multipurpose X-ray system-image quality and radiation exposure. Applied Sciences 10(17), 2020, 5876 [http://doi.org/10.3390/app10175876].

[20] Ott K.: Computed tomography of adult rhinosinusitis. Radiologic Technology 89(6), 2018, 571–593.

[21] Paul M. A. et al.: Assessment of functional rhinoplasty with spreader grafting using acoustic rhinomanometry and validated outcome measurements. Plastic and Reconstructive Surgery – Global Open. 6(3), 2018, p e1615 [http://doi.org/10.1097/GOX.0000000000001615].

[22] Pavlov S. V. et al.: Information Technology in Medical Diagnostics. CRC Press, 2017.

[23] Radulesco T. et al.: Correlations between computational fluid dynamics and clinical evaluation of nasal airway obstruction due to septal deviation: An observational study. Clinical Otolaryngology 44(4), 2019, 603–611 [http://doi.org/10.1111/coa.13344].

[24] Romanyuk S. et al.: Using lights in a volume-oriented rendering. Proc. of SPIE 10445, 2017, 104450U.

[25] Rovira J. R. et al.: Methods and resources for imaging polarimetry. Proc. of SPIE 8698, 2012, 86980T.

[26] Tang H. et al.: Dynamic Analysis of Airflow Features in a 3D Real-Anatomical Geometry of the Human Nasal Cavity. 15th Australasian Fluid Mechanics Conference, University of Sydney, Australia, 2004.

[27] Toriumi D.M.: Assessment of rhinoplasty techniques by overlay of before-and-after 3D images. Facial Plast Surg Clin North Am. 19(4), 2011, 711–723.

[28] Valtonen O. et al.: Three-dimensional printing of the nasal cavities for clinical experiments. Scientific Reports 10, 2020, 502 [http://doi.org/10.1038/s41598-020-57537-2].

[29] Vogt K., Jalowayski A. A.: 4-Phase-Rhinomanometry Basics and Practice. Rhinology 21, 2010, 1–50.

[30] Wójcik W., Pavlov S., Kalimoldayev M.: Information Technology in Medical Diagnostics II. London: Taylor & Francis Group, CRC Press, Balkema book, 2019.

[31] Zhang G. et al.: Correlation between subjective assessment and objective measurement of nasal obstruction. Zhonghua 43(7), 2008, 484–489.

D.Sc. Oleg Avrunin
e-mail: oleh.avrunin@nure.ua

Doctor of technical sciences, professor, Head of Biomedical Engineering Department, Kharkiv National University of Radio Electronics, Ukraine. Scientific supervisor of research work on research of theoretical and technical principles of diagnostics, assessment and correction of medical and social human conditions. Invited Professor in Gottfried Wilhelm Leibniz Universität Hannover (Germany) and Harbin Engineering University (China).

http://orcid.org/0000-0002-6312-687X

Oleksandr Avrunin
e-mail: oleksandr.avrunin@nure.ua

Student of the Department of Electronic Computers, Faculty of Computer Engineering, Kharkiv National University of Radio Electronics, Ukraine.
Research interests: information technologies in healthcare, signal processing and images, functional diagnostics of nasal breathing.

http://orcid.org/0000-0002-5202-0770

Ph.D. Yana Nosova
e-mail: yana.nosova@nure.ua

Ph.D., senior lecturer of the Department of Biomedical Engineering, Kharkiv National University of Radio Electronics, Ukraine. As part of the team of authors of the patent "Device for the testing of respiratory disorders of smell" was awarded the diploma of the winner of the All-Ukrainian contest "Invention of the Year – 2016" in the nomination "Best invention in Kharkiv region". Research Interests: biomedical signal processing and images.

http://orcid.org/0000-0003-4310-5833

Ph.D. Svetlana Kyrylashchuk
e-mail: ksa07750@gmail.com

Candidate of pedagogical sciences, Dean of the Faculty of Information Technologies and Computer Engineering, Associate Professor of the Higher Mathematics Department of the Vinnytsia National Technical University.
Scientific direction: methodology for the development of engineering thinking during the teaching of higher mathematics.

http://orcid.org/0000-0002-8972-3541

Ph.D. Nataliia Shushliapina
e-mail: schusha75@ukr.net

Ph.D., associate professor of Department of Otolaryngology, Kharkiv National Medical University.
Research interests: diagnostics of respiratory-olfactory disorders, functional chronology, connection of microcirculation with chronic diseases of the nasal cavity, computer planning of rhinosurgical interventions, intellectual training systems in otorhinolaryngology.

http://orcid.org/0000-0002-6347-3150

Ph.D. Olha Moskovchuk
e-mail: moskovchuk.olga11@gmail.com

Assistent, Ph.D., Vinnytsia Mykhailo Kotsiubynskyi State Pedagogical University, Department of Pedagogy, Professional Education and Management of Educational Institutions, Vinnitsa, Ukraine.
Research interests: information technology, methodology for the development of engineering thinking during the teaching of higher mathematics.

http://orcid.org/0000-0003-4568-1607

M.Sc. Ibrahim Younouss Abdelhamid
e-mail: ibrahim.younouss.abdelhamid@nure.ua

Ph.D. student, Department of Biomedical Engineering, Kharkiv National University of Radio Electronics.
Research interests: biomedical signal processing and images, functional diagnostics of nasal breathing.

http://orcid.org/0000-0003-2611-2417

Ph.D. Orken Mamyrbayev
e-mail: morkenj@mail.ru

Deputy General Director in science and Head of the Laboratory of Computer Engineering of Intelligent Systems at the Institute of Information and Computational Technologies of the Kazakh National Technical University named after K. I. Satbayev and associate professor in 2019 at the Institute of Information and Computational Technologies.
Main research field: machine learning, deep learning, and speech technologies.

http://orcid.org/0000-0001-8318-3794